

## BEHAVIOR OF HIGH STRENGTH STEEL FUSEIS SEISMIC RESISTANT SYSTEMS

Stella Avgerinou<sup>1</sup>, Ioannis Vayas<sup>1</sup>

<sup>1</sup>Institute of Steel Structures, National Technical University of Athens, Greece  
e-mail: [avgerinoustella@gmail.com](mailto:avgerinoustella@gmail.com), [vastahl@central.ntua.gr](mailto:vastahl@central.ntua.gr)

**Keywords:** High strength steel, Fuseis seismic resistant systems, RBS, Full scale tests

**Abstract.** *FUSEIS is an innovative seismic resistant system consisting of two closely spaced strong columns rigidly connected through multiple beams. The system resists lateral loads as a vertical Vierendeel beam. The dissipative elements are the FUSEIS beams and they usually have reduced beam sections (RBS) towards beam ends in order for the plastic hinge formation to be shifted away from the connections. In this paper, the behavior of a FUSEIS system with SHS and CHS beams made of high strength steel S700 is evaluated. The results of two full scale experimental investigations with different loading protocols are presented, together with corresponding numerical simulation. The tests were conducted in NTUA. Furthermore an application of the system in a four-storey building case study is presented along with the assessment of its behavior factor based on non-linear static and dynamic analyses.*

## 1 INTRODUCTION

Seismic resistant systems are those which provide lateral stability and hence seismic safety to a structure. The most common seismic resistant systems in steel structures are currently: moment resisting frames, concentric braced frames, eccentric braced frames and steel or composite vertical walls. Despite the structural efficiency of these conventional systems, their reparability after a strong earthquake is not equally advantageous. The FUSEIS on the other hand, is an innovative seismic resistant system with increased reparability while comparable to the conventional systems in terms of stiffness and ductility. The system was introduced and studied in the framework of a recent European Research Program named "FUSEIS" [8]. It is now further investigated with respect to its material properties in another European Research Program named "MATCH".

The system is composed by two strong columns rigidly connected by multiple beams. The beams run continuously from column to column or are cut in the middle and connected by short pins. The system resists lateral loads as a vertical Vierendeel beam mainly by combined bending and shear of the beams and axial forces of the columns. Considering a typical floor height of 3.4 m, four or five beams may be placed per storey. The seismic resistance of a building with Fuseis systems may be provided either by the systems alone or by a combination of their action with a moment resisting frame action. That depends on whether the beam-to-column connections of the structure are simple or rigid/semi-rigid. In order to prevent the transfer of moments to the foundations, the system's columns supports are formed as simple and also a fuse beam just above foundation level is used.

Modern seismic codes allow for the development of inelastic deformations in a structure's dissipative zones during the design earthquake. In case of a strong seismic event, the dissipative elements of the FUSEIS that can undergo damage up to a certain extent are the beams (or the pins) that thus constitute easily reparable fuses. In order for the plastic hinge formation to be shifted away from the beam-to-column joints the beams have reduced beam sections (RBS) towards their ends. The fuses-to-column connections must be designed with sufficient over-strength to achieve energy absorption only in the fuses and with bolted end-plates in order to enable the replacement of the fuses beams if needed. The fuses beam sections may be hollow or open and they also may vary between the floors of a multi-story structure following the increase of story shear or even vary within a story, leading to sequential plasticization of the fuses.

This study presents the results of two full scale tests on FUSEIS frames with hollow section beams. The beams material is high strength steel with nominal yield stress S700. The tests results are used for the development and calibration of simple FE models. Furthermore an example of the application of the system in a four-story structure is presented using fuses sections similar to those tested. The response of this case study is evaluated, using non-linear static and dynamic analyses.

## 2 DESCRIPTION OF TESTS

In total, eight FUSEIS full scale tests will be performed in the Institute of Steel Structures of the National Technical University of Athens in the context of the "MATCH" research program, in addition to the tests that were performed in the previous "Fuseis" research program [9],[10]. The parameters differentiating the various experimental investigations are the cross sections of the fuses, their materials and the loading protocols applied. In this paper the results of two tests with identical fuses beam specimens but different loading protocol are presented.

The experimental setup includes a rigid frame test rig available in NTUA's Laboratory, a computer controlled hydraulic cylinder and the test frame. The dimensions of the test frame

correspond to a real building frame: its height is 3.4m and the axial distance of the strong columns is 1.50m. The strong columns are rigidly connected by five fuses beams (Figure 3). The beam specimens were provided by RUUKKI-SSAB, a steel producer that focuses on high strength steel and also a participant in the research project. The beams have different cross sections along the height of the frame in order to achieve a sequential yielding of the specimens. All beam specimens have the same length and consist of hollow sections welded with identical plates at both ends. Bolted connections are used between the plates and the flanges of the strong columns in order to facilitate the replacement of the fuses after tests (Figure 1). Mounting of the test configuration is carried out with a crane due to the size and weight of the various parts. Aiming to shift the plastic hinge formation away from the beam-column connections, most of the specimens have reduced beam sections (RBS) towards their ends. The general properties of the fuses beams are summarized in Table 1. The steel grade of all beam specimens is S700 while the material of the end plates is S500. The yield stress of the material of the beams was provided by the steel producer and was specified as 790 MPa.

Cross section	Steel	Length (mm)	RBS
SHS 100*4	S700	722	yes
SHS 80*4	S700	722	yes
SHS 60*3	S700	722	no
CHS 76.1*3.2	S700	722	yes
CHS 60.3*4	S700	722	yes

Table 1: Summary of beam specimens



Figure 1: Fuses beam specimens

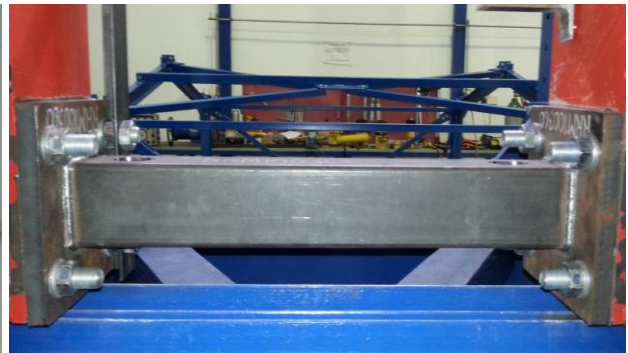


Figure 2: Bolted fuse beam

The columns of the test frame are connected to the rigid test rig by pin connections. At the bottom of the columns two UPN horizontal beams are connected at each side of the frame with pins in order to simulate the floor diaphragm at this level and assure equal displacements of the columns during the tests. In order to avoid displacements of the test frame in its out-of-plane direction, steel plates/leaders are used. The above details are depicted in Figure 3 and Figure 4.

Cyclic loading was applied through a hydraulic actuator positioned horizontally between the bottom of the columns and a base via two hinges. The actuator is computer controlled and its capacity is 500kN and 250mm back and forth. Both testing procedures are displacement controlled. The maximum drift of the frame reached in Test 1 is 4.8% while the (constant) maximum drift applied for Test 2 is 3.0%.

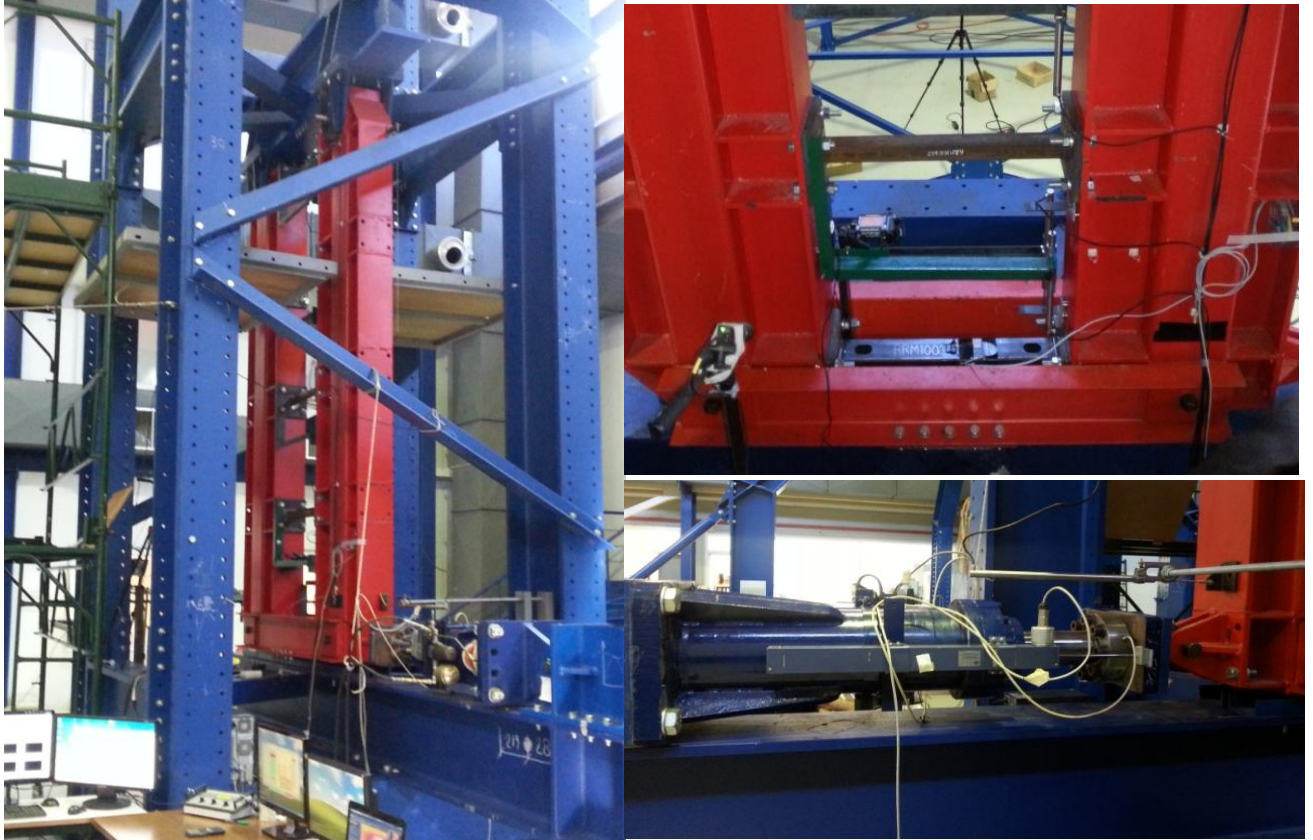


Figure 3: Experimental setup, test frame, “diaphragm” simulation and actuator



Figure 4: Pinned supports of columns steel leaders to avoid out-of-plane displacements

As far as the energy dissipation zones are concerned, the reduction of the fuses beam flanges at a certain distance from the connection areas was designed taking into account the EC8 and FEMA 350 recommendations [5],[16]. The selected reduced beam section properties are summarized in Table 2. The location and dimensions of the RBS are decided based on the following checks:

$$M_{cf,Ed} = (0.85 \div 1.00) * M_{pl,Rd,b} \quad (1)$$

$$V_{Ed,max} / N_{pl,rd} \leq 1.00 \quad (2)$$



where  $M_{cf,Ed}$  is the capacity design bending moment that develops at the column face when a plastic hinge forms at the centre of the RBS,  $M_{pl,Rd,b}$  is the beam plastic moment resistance away from the RBS,  $V_{Ed,max}$  is the capacity design shear force and  $V_{pl,rd}$  is the beam's shear force resistance.

	Distance a (mm)	RBS length (mm)	Flange reduction
FEMA 350	$0.5 \div 0.75 \cdot b_f$	$0.65 \div 0.85 \cdot h_b$	$< 0.50 \cdot b_f$
EC 8	$0.6 \cdot b_f$	$0.75 \cdot h_b$	$< 0.50 \cdot b_f$
SHS 100*4	50	60	$0.44 \cdot b_f$
SHS 80*4	50	60	$0.40 \cdot b_f$
SHS 60*3	-	-	-
CHS 76.1*3.2	50	50	-
CHS 60.3*4	50	50	-

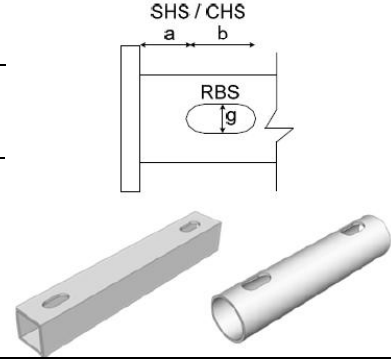


Table 2: Reduced beam sections

## 2.1 Loading procedures and data measurements

As mentioned above, the only difference between the two tests is the applied load protocol: in the first test the loading procedure has increasing amplitude and is based on the relevant ECCS recommendation [14] while in the second test a constant amplitude load protocol is applied. Both loading procedures are presented in Figure 5 and Figure 6 and Table 3. The required displacements are applied by the computer controlled hydraulic actuator with constant velocity 1.5mm/s. Short pauses are input between each cycle while longer pauses are input between cycles with increasing amplitude. The duration of each test was approximately 1.5 hours.

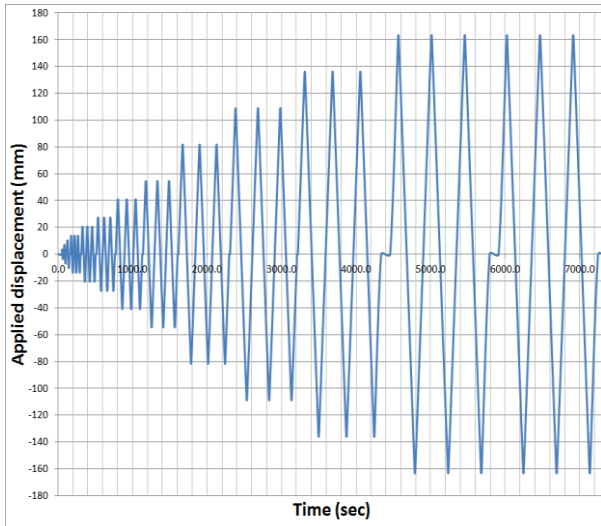


Figure 5: Load protocol for Test 1

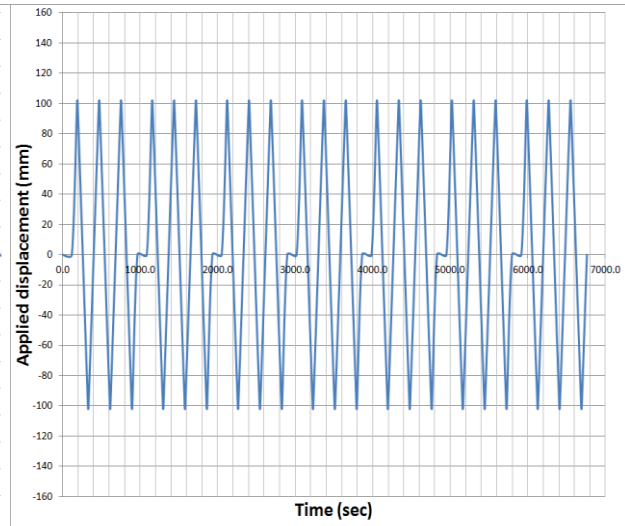


Figure 6: Load protocol for Test 2.

During the tests the following data were measured:

- Displacement of the actuator (controlled)
- Hydraulic load applied by the cylinder piston
- Differential displacement of beam ends in the direction vertical to the beams

- Displacement of the column connected with the actuator

Furthermore, a thermal camera was constantly recording one of the beam specimens.

Cycles	Test 1		Test 2	
	Displacement (mm)	Interstorey drift (%)	Displacement (mm)	Interstorey drift (%)
1	±3.4	±0.1	-	-
1	±6.8	±0.2	-	-
1	±10.2	±0.3	-	-
3	±13.6	±0.4	±102.0	±3.0
3	±20.4	±0.6	±102.0	±3.0
3	±27.2	±0.8	±102.0	±3.0
3	±40.8	±1.2	±102.0	±3.0
3	±54.4	±1.6	±102.0	±3.0
3	±81.6	±2.4	±102.0	±3.0
3	±108.8	±3.2	-	-
3	±136.0	±4.0	-	-
3	±163.2	±4.8	-	-

Table 3: Loading procedures of tests

## 2.2 Test results

In the following figures the test frame response curves (in terms of actuator force vs. frame drift) of the Fuseis systems are presented. As it can be noticed both tests were carried out until the frame strength dropped to less than 50% of its peak resistance. Load degradation occurred due to crack formation and opening and also due to local buckling. Plastic deformations took place within the fuses devices only.

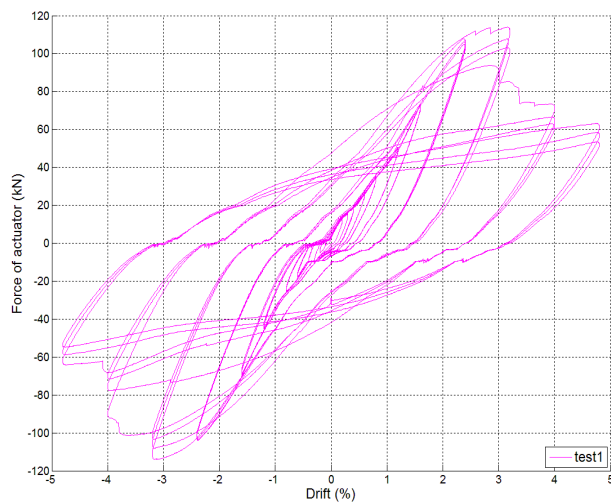


Figure 7: Frame response for Test 1

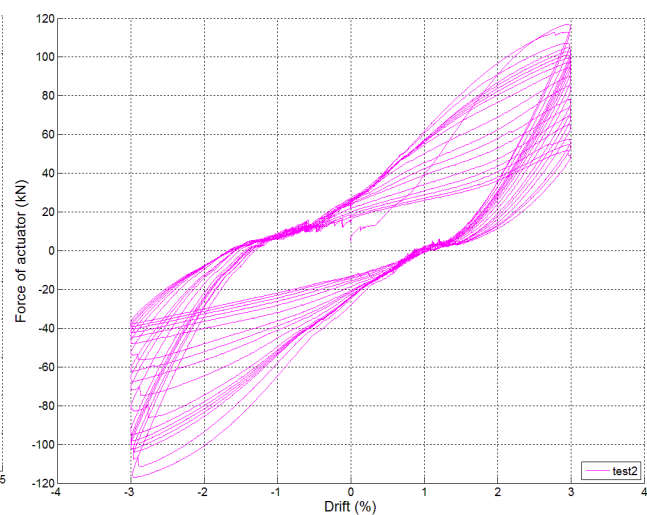


Figure 8: Frame response for Test 2.

Yielding of most specimens started at the reduced beams sections (RBS) area where eventually ductile fractures were observed. In the following figures the deformations as well as the failure of some specimens are presented indicatively.



Figure 9: (a) Cracks at RBS of a SHS beam and (b) at welds of a beam without RBS



Figure 10: (a) Cracks and (b) local buckling of CHS beam

The process of hinge formation in the reduced beam section area is shown in Figure 11 with snapshots of the thermal camera during the second (constant amplitude) test. The increase of temperature in the area of the RBS can be easily observed.

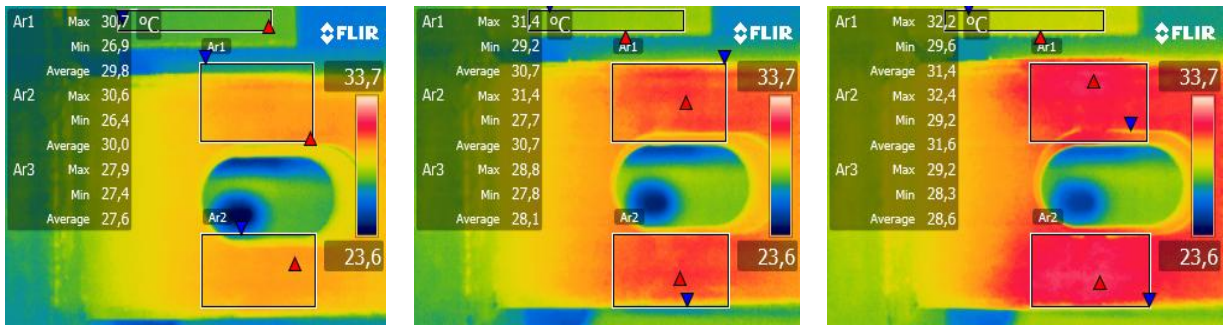


Figure 11: Thermal camera snapshots of a SHS during Test 2 in cycles 5,9 and 14 respectively.

The experimental investigations verified that the system behaves like a Vierendeel beam, resisting lateral loads by combined bending of the fuses and axial forces of the columns. Assuming that the hinges are formed in the midpoints of the reduced beam sections (and in case there are no RBS, they are formed at the beam end points), Figure 12 shows the theoretical static model of the frame and the forces equilibrium. The maximum theoretical story resistance ( $F_{theor}$ ) can be calculated as following:

$$F_{theor} = (2 \sum M_{pl,Rd,RBS} / l_{RBS}) * (L / h_{story}) \quad (3)$$

where  $L$  is the axial distance of the fuses columns and  $l_{RBS}$  is the distance of the midpoints of the reduced beam sections.

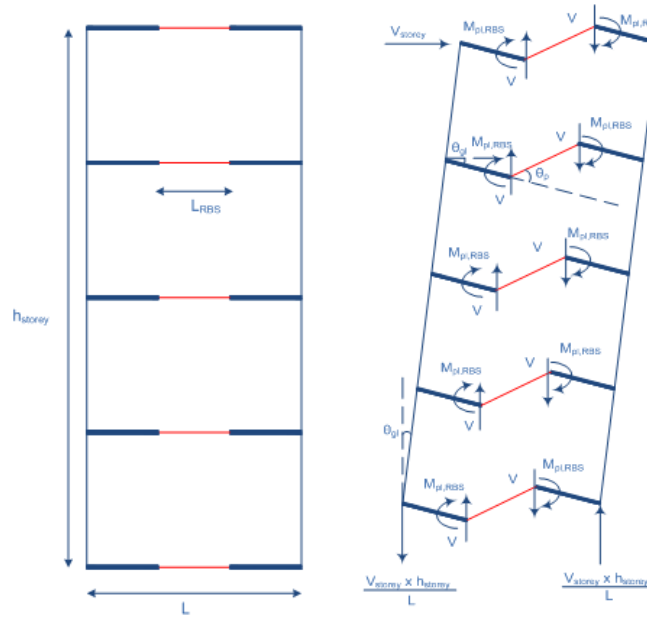


Figure 12: Static system and force/moments equilibrium

Table 4 shows the theoretical force as derived from eq. (3), together with the maximum forces achieved by the tests. The good relation indicates that the Vierendeel model describes well the ultimate capacity of the system. The table shows also the ultimate rotations and number of cycles achieved during the two tests. Two values of this rotation are given that correspond to different failure criteria: The first criterion represents the 20% reduction of the maximum strength and/or initial stiffness and the second criterion relates to 80% of the theoretical value  $F_{theor}$ . While for the first test -which was performed with increasing displacements- the failure criterion is stated in terms of drifts, in the second test -which had constant amplitude- failure is presented in terms of cycles (Table 4).

Test	Load Prot.	$F_{max}$ (kN)	$F_{theor}$ (kN)	$F_{max}/F_{theor}$	crit.1	crit.2
T1	ECCS	113	113	1.00	$\theta=0.034$	$\theta=0.034$
T2	const.ampl.	117	113	1.04	N=8	N=10

Table 4: Comparison between maximum frame resistance and theoretical force

### 2.3 Calibration of simple test model in SAP

The relatively common software SAP2000 is selected in order to form a simple model that approaches the behaviour of the Fuseis test frames. The fuses beams are simulated with appropriate beam finite elements. Their net length is subdivided to five zones representing the full sections and the reduced beam sections (RBS). Rigid zones are assigned from column centres to column faces. Aiming to match the initial stiffness of the model frame with its experimental elastic stiffness, rotational links were used in the position of the bolted end plates of the fuses beams and stiff translational springs are used (Figure 13).

The response of the model frame under lateral loading is evaluated using non-linear incremental static analysis. The pushover's target displacement corresponds to the maximum displacement applied by the actuator on the test frames. Having located the energy dissipation zones on the fuses during the experimental investigations, hinges were assigned respectively. More specifically regarding the RBS elements, plastic hinges were located in their middle.



The moments and rotations required to describe the non-linear behaviour of each fuse were calculated using the following equations:

$$M_{pl,RBS} = W_{pl,RBS} * f_y \text{ and } M_{y,RBS} = M_{pl,RBS} / a_{pl} \quad (4)$$

$$\theta_y = M_y * l_b / (6 * E * I_y) \quad (5)$$

The definition of the moment-rotation hinge properties was approached through comparison with the experimental data but remain to be verified with additional numerical and experimental investigations.

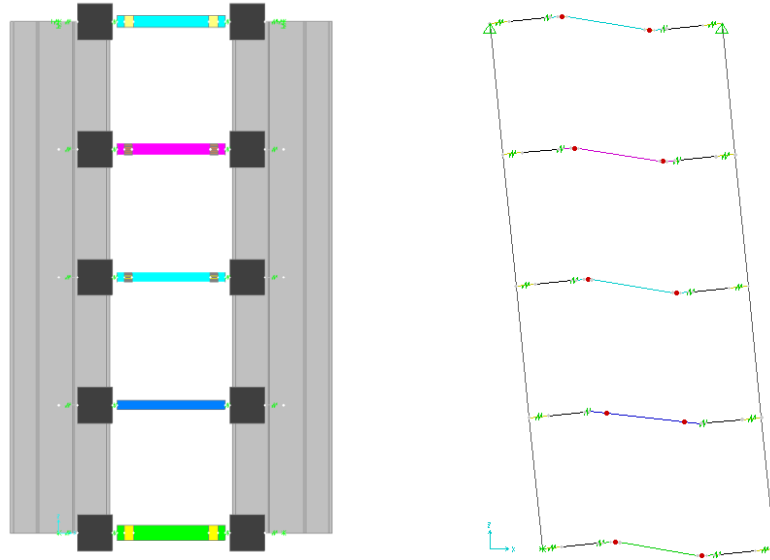


Figure 13: SAP model, pushover deformation and plastic hinge formation

The pushover curve of the model is compared with the positive and negative skeleton curves derived from Test 1 (Figure 14).

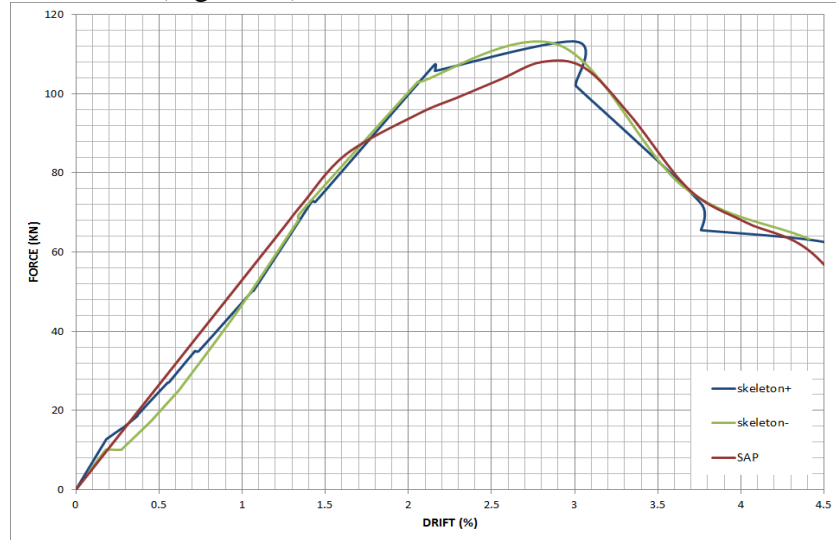


Figure 14: Comparison of pushover with skeleton curve for test calibration

### 3 DESIGN OF A MULTI-STORY BUILDING FRAME WITH FUSEIS

Based on the feedback from the experimental investigations, a four-storey building with Fuseis systems was designed using the SAP2000 software. The dimensions of the 2D frame are typical: the storey height is 3.4m and the span length is 7.0m. The axial distance of the

Fuseis strong columns is 1.50m (Figure 15). The loads applied are representative for office or residential buildings according to EC1 [1] while the effective width for the loads in the transverse direction of the frame is assumed 6.0m. Composite action is taken into account, assuming composite decks consisting of profiled steel sheeting. The effective widths as well as the equivalent lengths of the composite beams were calculated according to EC4 [3]. Composite beam sections are simulated by adversely taking into account only the participation of the concrete above the profiled sheeting. The general assumptions for the design of the buildings in terms of materials, vertical loads and seismic parameters are displayed in Table 5.

Materials	
Steel members	S355
Fuses beams	S700
Vertical loads	
Dead (slabs)	2.2 kN/m <sup>2</sup>
Additional dead	2.0 kN/m <sup>2</sup>
Imposed loads	3.0 kN/m <sup>2</sup>
Seismic parameters	
Type of spectrum	EC8, Type 1
PGA	0.25g
Importance class	II, $\gamma=1.00$
Ground /Soil	Type B, $S=1.2$
Behaviour factor $q_{des}$	5.00
Factors $\phi$ (EC8,p.1, 4.2.4)	$\phi = 1.00$ (roof) $\phi = 0.80$

Table 5: General assumptions for the design of the case study

The design of the building was according to the provisions of EC3, EC4 and EC8 [1],[2],[3],[4],[5]. Additional rules given in the FUSEIS Design Guide [7] were applied to ensure that yielding, takes place in the FUSEIS beams prior to any yielding or failure elsewhere. The sections of the fuses beams used in the design were chosen amongst the types tested. However, the specific sections chosen as well as the required number of the FUSEIS systems was mainly determined by the limitations of inter-storey drifts ( $dr*v < 0.0075*H$ , for buildings with ductile non-structural members) and second order effects.

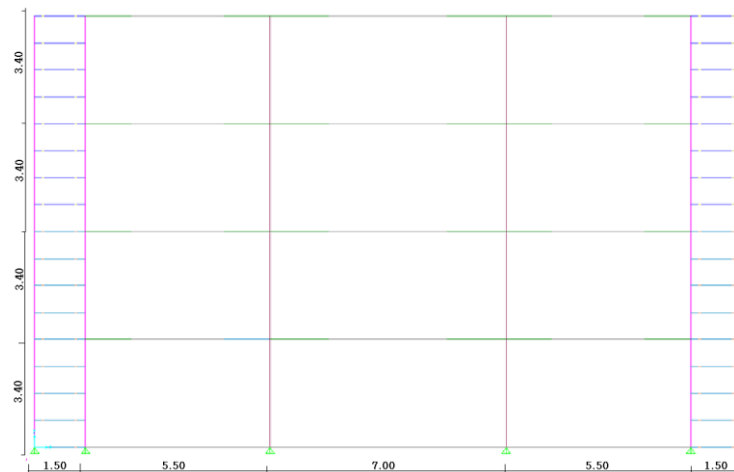


Figure 15: model of the 4story frame in SAP

As far as the beam-to-column connections are concerned, in this case they were chosen to be semi rigid which means that the Fuseis systems are combined with the overall moment resisting frame to provide the seismic resistance of the building.

Regarding the modal analysis, the period of the first mode of vibration is 1.3sec and the mass participation ratio exceeds 88%. One more mode is needed for the activation of 97% of the mass while the respective percentage required by codes is 90%.

#### 4 NON-LINEAR STATIC ANALYSIS AND EVALUATION OF THE BEHAVIOUR FACTOR

For further investigation of the case study's seismic behaviour, non-linear static analysis was performed. The scope was to quantify the structure's maximum base shear capacity and the ultimate displacement and eventually calculate the behaviour, ductility and overstrength factors. The analysis was performed under displacement control and the maximum displacement applied on the top floor translated to an average building drift equal to 6%. Two types of vertical distribution of the lateral load were used: one with uniform pattern and another proportionate to the fundamental modal shape (inverted triangle). These two types in a way represent an upper and a lower limit for the structure's response (Figure 17). While the lateral loads increased monotonically, the gravity loads remained constant ( $1.0 \cdot G + 0.3 \cdot \phi \cdot Q$ ). Second order effects were taken into account.

In order to simulate material non-linearity, potential plastic hinges were assigned in all areas prone to exhibiting very large deformations or inelastic behaviour. More specifically plastic hinges were located in the middle of the fuses reduced beam sections (RBS), at the beams close to the beam-to-column connections and at selected areas of the columns. While the columns were assigned with automatic hinges taking into account the interaction between axial forces and bending moments, the beams and the fuses RBS were assigned with user defined moment-rotation hinges. The simulation of the behaviour of the fuses hinges was based on the results of the test's calibration presented above.

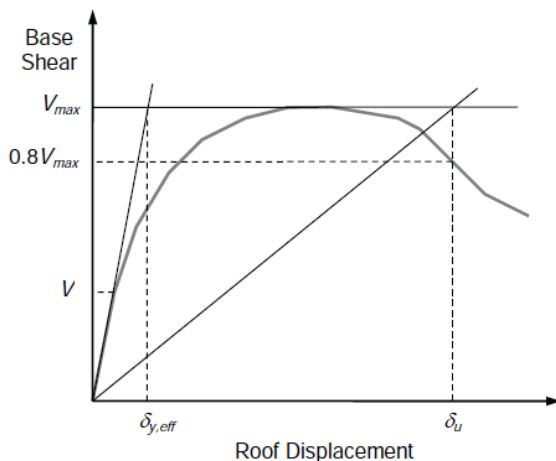


Figure 16: Idealized pushover curve (FEMA695)

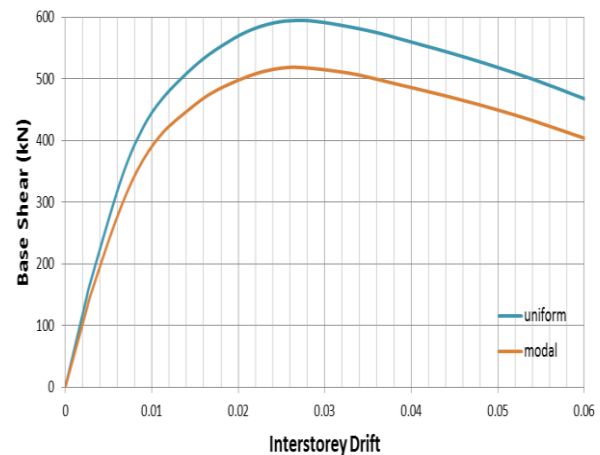


Figure 17: Pushover curves for "uniform" and "modal shape" lateral load distribution

In order to evaluate the structure's behaviour factor the product of overstrength and ductility must be calculated. The overstrength of the structure is defined as the ratio of the maximum base shear resistance on the pushover curve over the base shear at first (fuse) yield ( $\Omega = V_{max}/V_I$ ). Ductility is defined as the ratio of the ultimate roof displacement over the effective yield displacement ( $\mu = \delta_u/\delta_{y,eff}$ ) (Figure 16). The ultimate roof displacement may be assumed to represent either the point of 20% strength loss ( $\delta_u$ ) or a point at which another non-

simulated failure mode occurs such as for example, the failure mode indicated by the experimental investigations ( $\delta_{uexp}$ ) (Figure 18)[6]. In Table 6 the results of the pushover analysis are summarized. Calculations were based on the pushover analysis with uniform lateral load distribution. The performance point is also presented according to ATC-40 provisions [15]. It should be noted that the values of the factors presented need further recalculation to take better into account the additional future experimental results and respective numerical simulations.

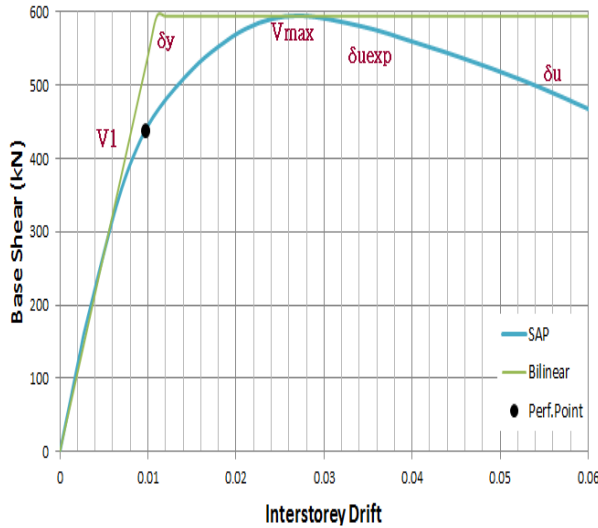
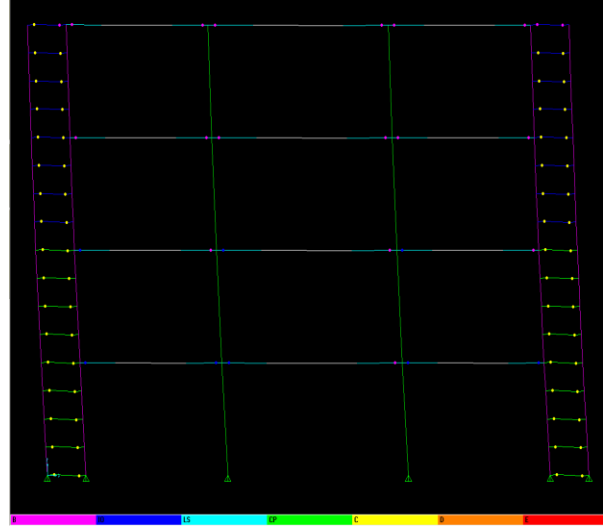


Figure 18: Pushover curve and bilinear approach

Figure 19: Deformed frame at  $\delta_u$  and hinge formation

$\mu = \delta_u / \delta_y$	$\mu_{exp} = \delta_{uexp} / \delta_y$	$\Omega = V_{max} / V_1$	$q = \mu * \Omega$	$q_{exp} = \mu_{exp} * \Omega$
5.1	3.1	1.4	7.3	4.4

Table 6: Calculation of  $\mu, \Omega$  and  $q$  factors

## 5 NON-LINEAR DYNAMIC ANALYSIS AND PERFORMANCE ASSESSMENT

Non-linear dynamic analysis was performed on the four-story case study using the Far-Field Real Accelerograms set suggested by FEMA provisions [6]. This set includes 22 records (44 individual components) taken from 14 strong seismic events that have occurred around the world during the last decades (events with average magnitude of M7.0 and average site-source distance 16.4km). The analysis was performed using OpenSees software.

The scaling factors used for Incremental Dynamic Analysis (IDA) were obtained by dividing the desirable level of acceleration over the first mode spectral acceleration for each accelerograms input ( $Sa(T_1)$ ). In this case, 20 scaling factors were used ranging from 0.1g up to 2.0g, aiming to cover the range from elastic behaviour to collapse. In order to describe the scaling of each ground motion record and the structural response, an intensity measure (IM) and a damage measure (DM) were introduced respectively. For each ground motion record and every iteration the overall maximum (absolute) inter-story drift was selected and thus the IDA curve was produced.

Generally, the IDA study is accelerogram and structural model specific, therefore the differences between the various IDA curves represent the differences of the structure's response when subjected to earthquakes with different frequency characteristics [11],[12]. As it can be seen in Figure 20, all curves exhibit a distinct elastic linear region that ends when the first nonlinearity occurs. IDA curves terminate at different levels of acceleration with a final soft-



tening segment (“flatline”) which indicates increasingly high accumulation of DM and signals dynamic instability.

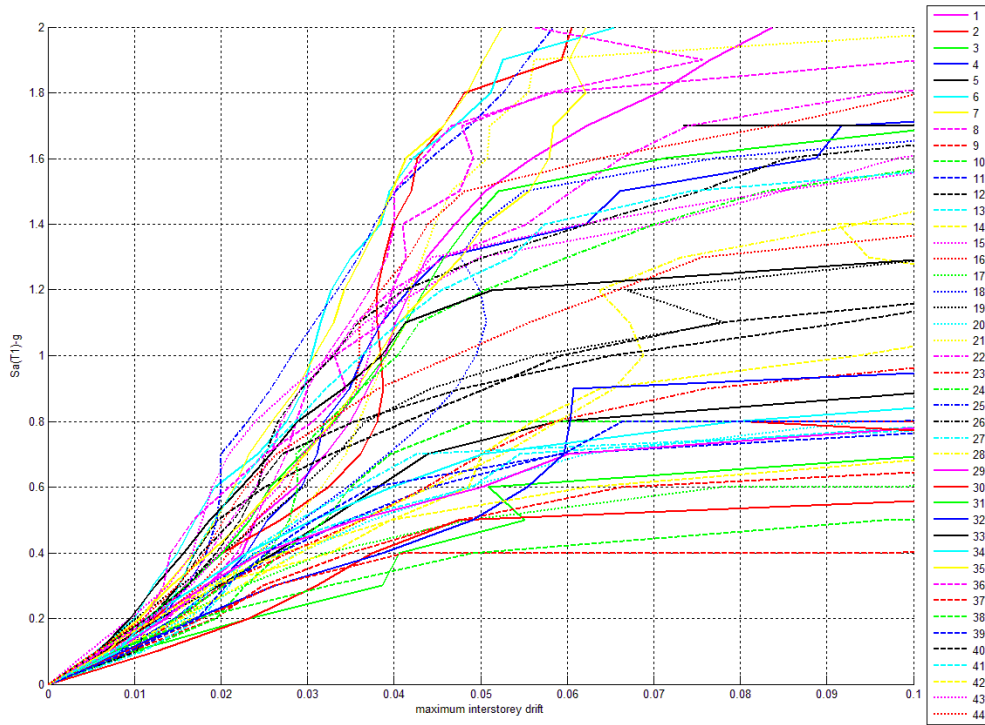


Figure 20: 44 IDA curves (FEMA Far-Field Record Set)

For a better evaluation of the IDA results, the 16%, 50% and 84% fractile curves were calculated. The flatline of the 50% fractile (median curve) represents the median collapse intensity  $S_{CT}$ . The Collapse Margin Ratio (CMR) is used to characterize the collapse safety of the structure and is calculated as the ratio of the median collapse capacity  $S_{CT}$  over the intensity of the maximum considered earthquake  $S_{MT}$ . [12][13]

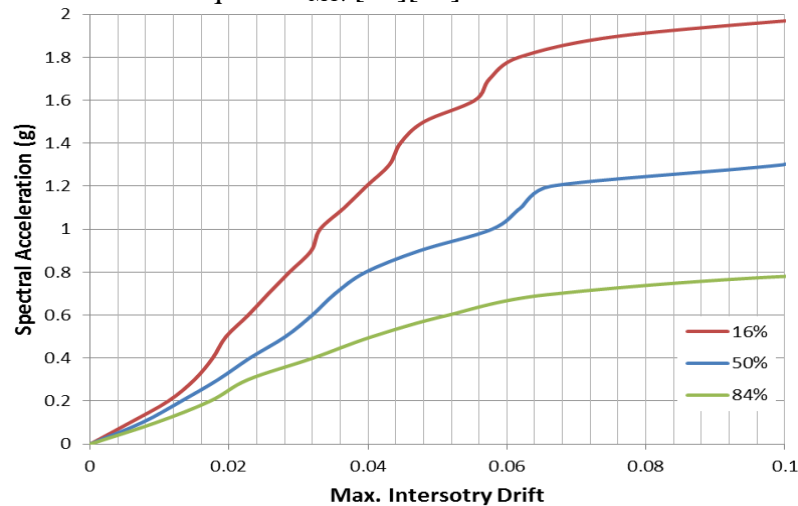


Figure 21: IDA fractiles (16%, 50% and 84%)

Collapse for a ground motion is judged to occur either directly from dynamic analysis (existence of “flatlines”) or assessed indirectly through non-simulated component limit state criteria. The results of the IDA can be then summarized using a fragility function which describes probability of the defined collapse as a function of an earthquake’s intensity (accel-

eration level) [6]. In this case, fragility curves are drawn by assuming two types of failure: (a) collapse due to excessive lateral displacements (flatlines) and (b) a non-simulated collapse due to exceedance of the drift representing a selected Limit State (Figure 22). More specifically, non-simulated collapse is assumed to occur at drifts beyond 3.4% which corresponds to 20% strength loss of the Fuseis system as indicated by the experimental investigations. Both collapse fragility curves were defined by a cumulative lognormal distribution function and were fitted to the points representing the aforementioned failure criteria. The parameters required for the definition of these functions were the median collapse intensity  $S_{CT}$  and a factor  $\beta$  representing dispersion in results due to uncertainties, for each case.

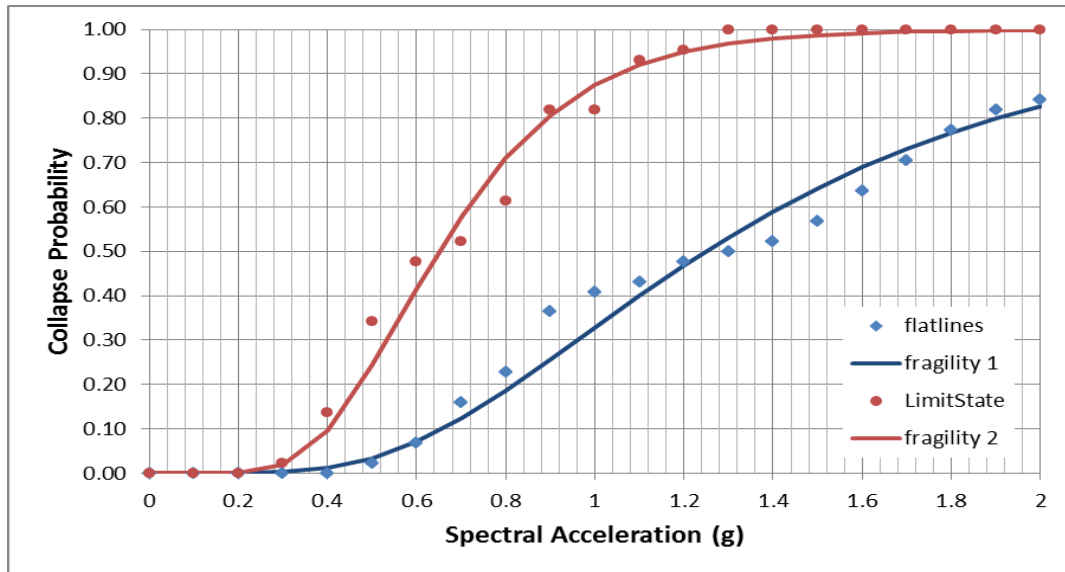


Figure 22: Fragility curves for simulated and non-simulated failure modes

As far as performance evaluation is concerned, the methodology suggested by FEMA 695 is followed (Table 7) [6]. First, CMR is subjected to spectral shape adjustment by means of the SSF (spectral shape factor) which is a function of the fundamental period  $T$  and the structures ductility  $\mu$  ( $ACMR = CMR * CCF$ ). This adjustment is to assure that the peaked spectral shapes of the rare ground motions used in IDA are not less damaging than a standard design spectrum. Then acceptability is measured by comparing the ACMR to the acceptable values of  $ACMR_{10\%}$  that depend on the systems uncertainties ( $\beta$ ).

Collapse type	$S_{CT}$	CMR	ACMR	$ACMR_{10\%}$
Sidesway (flatline)	1.25	2.90	3.87	1.90
Non-simulated	0.65	1.50	2.01	1.62

Table 7: Assessment of collapse performance according to FEMA695

As it can be observed in Figure 22 and Table 7, in case collapse is defined by non-simulated limit state criteria, the probability of collapse for a certain level of acceleration is significantly increased while the Collapse Margin Ratio (CMR) is reduced likewise. However in both cases, the acceptance criterion was satisfied.

## 6 CONCLUSIONS

- Innovative fuses systems may be applied to multi-storey steel buildings as an alternative to conventional seismic resistant systems. They combine ductility, architectural versatility, stiffness and reparability.
- The system is composed of two closely spaced columns rigidly connected with multiple short beams that are its dissipative elements.
- As an extension to previous research, experimental and analytical/numerical investigations have been carried out where the dissipative beams are of high strength steel S 700.
- Results indicate that the system with high strength beams still shows ductility, together with strength and stiffness and could be used in seismic regions.

## 7 ACKNOWLEDGEMENTS

The research presented is made in the framework of the European Research Project RFSR-CT-2013-00024: “Material Choice for Seismic Resistant Structures (MATCH)”. The financial contribution of the Research Fund for Coal and Steel of the European Community is greatly acknowledged. The other partners of the project are: RWTH Aachen (coordinator), University of Pisa, University of Thessaly, RUUKKI-SSAB metals Oy and ILVA Spa.

## REFERENCES

- [1] Eurocode 1: Actions on structures - Part 1-1: General actions - Densities, self-weight, imposed loads for buildings; EN 1991-1-1:2002
- [2] Eurocode 3: Design of steel structures - Part 1-1: General rules and rules for buildings; EN 1993-1-1:2005
- [3] Eurocode 4: Design of composite steel and concrete structures - Part 1-1: General rules and rules for buildings; EN 1994-1-1:2004
- [4] Eurocode 8: Design of structures for earthquake resistance - Part 1: General rules, seismic actions and rules for buildings; EN 1998
- [5] Eurocode 8: Design of structures for earthquake resistance - Part 3: Assessment and Retrofitting of buildings; EN 1998-3:2004
- [6] FEMA P695: Quantification of building seismic performance factors, 2009.
- [7] Vayas, Ph. Karydakis, D. Dimakogianni, G. Dougka, C.A. Castiglioni, A. Kanyilmaz, B. Hoffmeister, T. Rauert, et al, “Dissipative devices for seismic resistant steel frames – The FUSEIS project, Design guide”. Research Programme of the Research Fund for Coal and Steel, 2012.
- [8] Vayas, Ph. Karydakis, D. Dimakogianni, G. Dougka, C.A. Castiglioni, A. Kanyilmaz, B. Hoffmeister, T. Rauert, et al, “Dissipative devices for seismic resistant steel frames – The FUSEIS project, Final Report”. Research Programme of the Research Fund for Coal and Steel, 2012.

- [9] Dougka, G., Dimakogianni, D., Vayas, (in press) I. Innovative energy dissipation systems (FUSEIS 1-1) - Experimental analysis. *Journal of Constructional Steel Research*, Vol. 96 (5), pp 69-80, 2014
- [10] Dimakogianni, D., Dougka, G., Vayas, I. Innovative seismic-resistant steel frames (FUSEIS 1-2) experimental analysis. *Steel Construction Design and Research*, Vol. 5 (4), pp. 212-221, 2012.
- [11] Vamvatsikos D., Cornell C.A, 2002, "Incremental Dynamic Analysis", *Earthquake Engineering & Structural Dynamics*, John Wiley & Sons, Ltd.
- [12] Vamvatsikos D., Cornell C.A, 2005, "Seismic Performance, capacity and reliability of structures as seen through Incremental Dynamic Analysis", *The John A. Blume Earthquake Engineering Center*, Stanford University
- [13] ASCE Standard 7-05: Minimum Design Loads for Buildings and Other Structures, American Society of Civil Engineers, 2006
- [14] ECCS: Recommended testing procedure for assessing the behaviour of structural steel elements under cyclic loads. Technical committee 1: structural safety and loadings, technical working group 1.3: seismic design, 1986
- [15] ATC 40: Seismic evaluation and retrofit of concrete buildings, Applied Technology Council, California Seismic Safety Commission, 1996
- [16] FEMA 350: Recommended seismic design criteria for new steel moment frame buildings, 2000.